Scientific Research Publishing

Open Journal of Geology, 2026, 16(1), 12-34
https://www.scirp.org/journal/ojg
ISSN Online: 2161-7589
ISSN Print: 2161-7570

A Toposequential Study of Duricrusts Developed on Granite and Gneiss in Meiganga, Adamawa Region: Understanding Lateritic Formations Assessment in Central Cameroon

Tatuebu Tchuenguem Fritz[1], Sini André[1,2*], Djetenbe Beral[1], Tchoukeu Yvests Briault[1], Welba Moise[3], Nguetnkam Jean Pierre[1], Mapongmetsem Pierre Marie[4]

[1]Department of Earth Sciences, Faculty of Science, University of Ngaoundere, Ngaoundere, Cameroon
[2]Department of Mining Engineering, School of Geology and Mining Engineering, University of Ngaoundere, Ngaoundere, Cameroon
[3]Department of Earth Sciences, University of Yaounde 1, Yaounde, Cameroon
[4]Department of Biological Sciences, Faculty of Science, University of Ngaoundere, Ngaoundere, Cameroon
Email: *andrsini@yahoo.com

How to cite this paper: Fritz, T.T., André, S., Beral, D., Briault, T.Y., Moise, W., Pierre, N.J. and Marie, M.P. (2026) A Toposequential Study of Duricrusts Developed on Granite and Gneiss in Meiganga, Adamawa Region: Understanding Lateritic Formations Assessment in Central Cameroon. *Open Journal of Geology*, **16**, 12-34.
https://doi.org/10.4236/ojg.2026.161002

Received: December 19, 2025
Accepted: January 24, 2026
Published: January 27, 2026

Abstract

This study investigates the toposequential development of duricrusts formed on granite and gneiss in Meiganga, in the Adamawa Region of Central Cameroon. The area lies within a tropical upland characterized by duricrust outcrops. The methodology includes field investigations for duricrusts description and sampling for mineralogically and geochemically characterizations. Eleven samples were collected including six on granite and five on gneiss. Four main facies were identified: nodular and massive at both sites, vacuolar exclusively on granite, and brecciated only on gneiss. The study reveals a toposequential differentiation of the duricrusts with high-altitude positions (1150 m) displaying thick and mature duricrusts enriched in goethite and gibbsite, while mid and lower slope sites (1000 - 1050) show less indurated and kaolinite-rich materials. Geochemically, Fe_2O_3, the most important oxide, varied from 28.62% to 78.79%. It is followed by Al_2O_3 (3.06% - 32.6%). The SiO_2 contents ranged from 0.95% to 22.48%. The alkali and alkaline earth elements are mostly low (0.1%). Most important trace elements identified are Ba (5 - 1191 ppm), V (108 - 1118 ppm) and Zr (9.6 - 529.4 ppm). LREE are more concentrated than HREE: 459.57 ppm and 39.44 ppm for granitic duricrusts; 722.45 ppm and 54.86 ppm for gneissic materials. The high CIA and MIA values (>99) confirm an intense duricrust weathering, leading to clay minerals development through ferruginization, monosialitization, and allitization. These re-

sults support a model of lateritic landscape evolution based on topography, lithology, and climatic conditions, which favored the understanding of duricrust processes in general and those of Adamawa region in particular.

Keywords

Adamawa Highlands, Meiganga Locality, Duricrust Development, Mineralogical and Geochemical Investigations, Crystallochemical Phenomena

1. Introduction

Lateritic duricrusts play an important role in the landscapes of tropical Africa [1]-[3]. They result from the physical and chemical rocks alteration, with the release of less mobile chemical elements that need to recrystallize into indurated materials rich in oxides and hydroxides of iron, aluminum, and sometimes manganese and titanium [4]. These formations frequently display high concentrations of metals and therefore can constitute economic resources for the development of countries [5] [6].

Cameroon, located in an intertropical zone, has a diversity of climates ranging from equatorial in the south to Sudano-Sahelian in the north and far north regions [7]. This climatic variability, associated with rock properties, has an influence on alteration processes. These lead to the mobilization and the concentration of chemical elements on the Earth's surface [8] [9], promoting the development of duricrust materials. Several researchers have carried out detailed studies on morphological, mineralogical, and geochemical features of duricrusts throughout Cameroon, but most of them have been conducted in the western part of the country [8] [10] [11] and in the Adamawa region [12] [13]. Some of these studies have provided important insights into the processes governing duricrust development in tropical environments, highlighting the importance of topographical factors [14].

These materials are therefore becoming potential resources that require further investigations in order to deepen knowledge of them across the Adamawa region. The southern part of Meiganga, located in the Adamawa region, rests on a crystalline basement mainly composed of granitic and gneiss rocks. The region displays a landscape of uplands with high plateaus, mid-slopes, and lower pediments, offering a natural gradient for the spatial evolution of weathering products.

This study focuses on investigating the toposequential evolution of duricrusts along this geomorphic gradient, aiming to identify the morphological, mineralogical, and geochemical changes linked to their position on the landscape and underlying lithology. The results should support regional models of landscape evolution and provide insights into the climatic and geomorphological conditions that shaped the current duricrust landforms in the Adamawa region.

2. Materials and Methods

2.1. Study Area and Geological Settings

The study is carried out in Meiganga, located at latitudes 06˚45' and 06˚30' north and longitudes 14˚00' and 14˚45' east (Figure 1). It is characterized by a Sudano-Guinean climate, which is intermediate between the wetter south of Cameroon and the relatively dry north, with two distinct seasons: a dry season from November to April and a rainy season from May to September. It has a Sudano-Guinean climate, intermediate between the more humid south of Cameroon and the relatively dry north, with two distinct seasons: a dry season from November to March and a rainy season from April to October. Annual rainfall ranges from 1500 to 1700 mm. Depending on the climate, parent materials and topography, several types of soils are found. They include ferruginous, ferralitic and hydromorph soils [15] [16]. These soils support Sudano-Guinean savanna vegetation significantly affected by human activities [17]. Three of the four major river basins in Cameroon have their origin in Adamawa: The Atlantic basin, the Lake Chad basin, and the Niger basin. The study area is traversed by some dendritic watercourses, including permanent ones that often mark the limits of the lowlands. The region's orography is divided into two main units: one with altitudes between 1000 and 1100 m and the other with altitudes between 1100 and 1150 m.

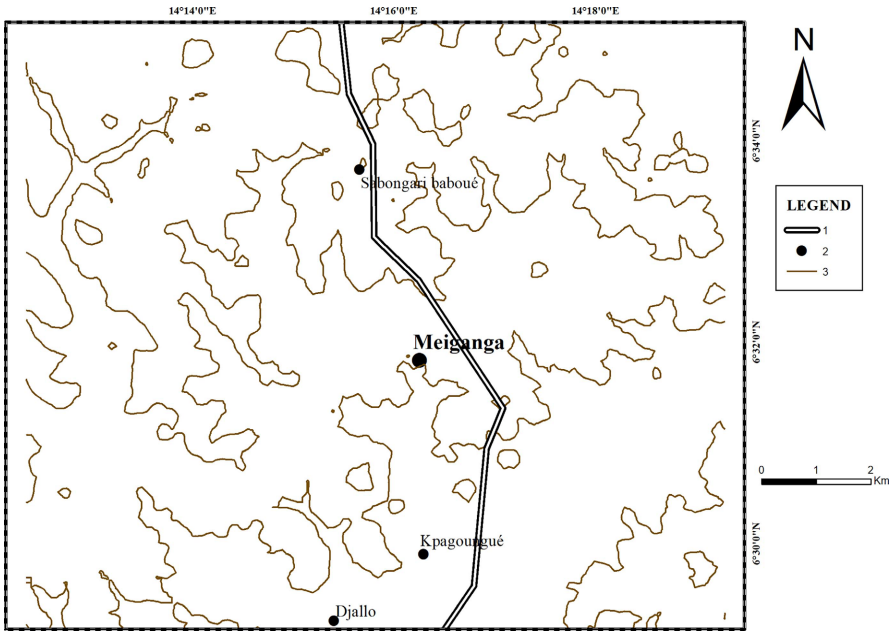

Figure 1. Location map of the study area. (a) Map of Cameroon in Africa; (b) Administrative map of Cameroon showing the study area in the Adamawa region; (c) Study area; (1) Main Road; (2) Locality; (3) Level curve.

The geology (Figure 2) is based on a bedrock of metamorphic rocks and granitoids of Pan-African orogenesis [18] [19], crossed by a series of major faults [20]. The volcanic activity in the region is probably associated with the Pan-African

fractures affecting the northern, eastern, and southern areas of the Adamawa Plateau [21]. The morphology of the highlands resulted from the complex tectonic processes, combining uplifts and subsidence with intense magmatic activity. These events, which occurred during the Mesozoic and Cenozoic eras, caused major fractures in the Precambrian basement [21].

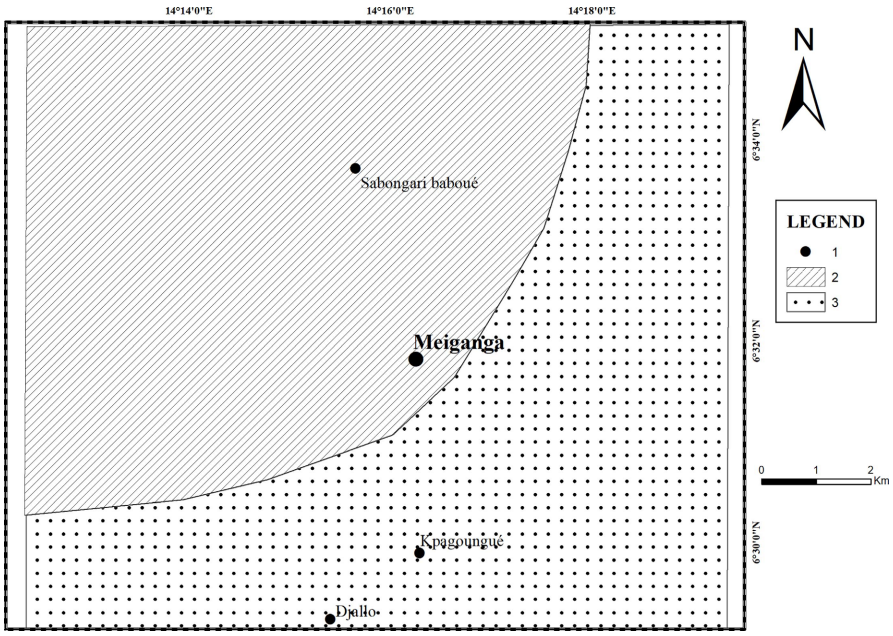

Figure 2. Geological map. (1) Locality; (2) Gneissic formations; (3) Granitic formations.

2.2. Sampling and Methods

Both sites investigated are shown in **Figure 3** which clearly indicates the two units of altitude involved, consisting of eleven samples, six from granite (E06, E07, E08, E09, E10 and E11) with altitude 1000 to 1100 m and five from gneiss (E01, E02, E03, E04 and E05) with altitude 1100 to 1150 m. Sampling was carried out on the basis of duricrust facies constituted of nodular, massive, vacuolar and brecciated, coupled with their outcrops at hilltop (E04, E05, E06 and E07), at mid-slope (E03, E08, E09 and E10), and at the bottom of the hill (E01, E02 and E11) depending on whether the sample was taken from granite or gneiss. All the samples were analyzed mineralogically to identify the duricrust mineral phases and geochemically to determine different minerals constituted (major, trace and rare earth elements).

2.3. Analytical Techniques

The sample preparation was carried out at the Mechanical Ore Preparation Laboratory of the School of Geology and Mining of Meiganga. The mineralogical analyses were conducted at the Soil Chemistry Laboratory of the University of Johannesburg in South Africa. It was supplemented by geochemical analyses at the Bureau Veritas Mineral Laboratory in Canada. During the sample processing, the procedure uses a jaw crusher with steel plates. Subsequently, a ball mill was

used to pulverize the samples. The fraction less than 100 µm was used for analysis. The chondrite-normalized samples were implemented according to [22].

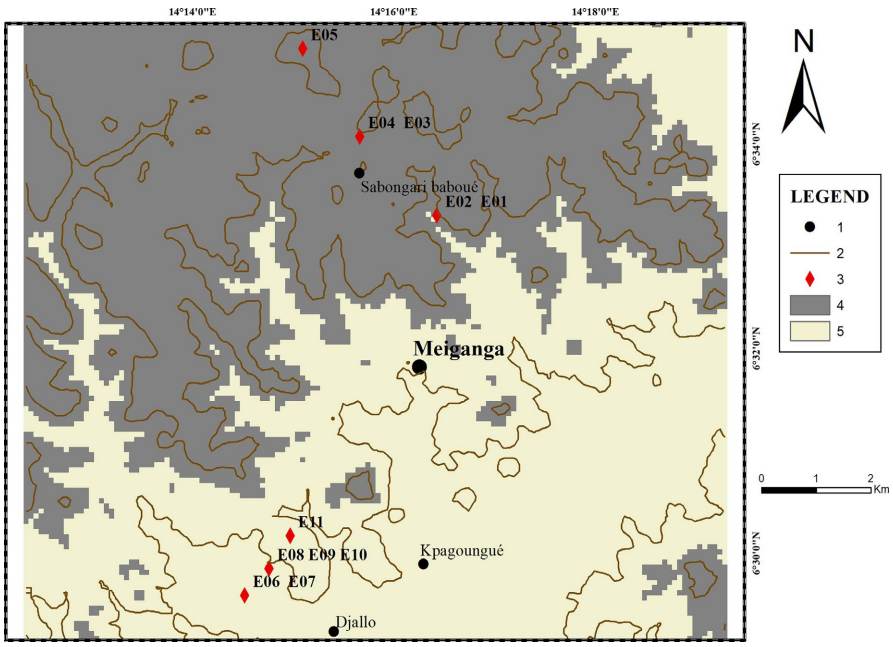

Figure 3. Sampling map indicating the two sites of duricrust outcropping: (1) Locality; (2) Level curve; (3) Sampling point; (4) Gneissic zone with 1000 to 1050 m of altitude; (5) Granitic zone with 1100 to1150 m of altitude.

X-ray diffraction (XRD-100) was performed for mineralogical analysis. The sample powders were ground with an agate mortar and pestle, and smear mounts were prepared on low-background silicon discs for analysis. The samples were analyzed with Co radiation at 40 kV and 45 mA. The following parameters were used in the X'Pert HighScore Plus software for peak identification: minimum significance: 1.00; minimum peak width (˚2θ): 0.01; maximum peak width (˚2θ): 1.00; peak base width (˚2θ): 2.00; Method: Smoothed peak top. A refinement process was also applied to semi-quantify the proportion (%) of each mineral. Each mineral proportion is obtained by the ratio between the surface area of the XRD peaks specific to each mineral and the total surface area of the XRD pattern of the sample. The method is accurate over a wide range of concentrations (up to 100% oxide) for many elements and provides results that fall within the limits of the accepted published uncertainties for a wide range of CRM.

Wavelength Dispersive X-ray Fluorescence Spectrometry (WD-XRF) was used for the determination of major elements. This analytical procedure was complemented by the use of the ICP-AES methodology (Model IAT-100). In order to maintain the high quality of routine analyses, calibration maintenance, examination of calibration robustness, and verification of lower detection limits (LDL) must be performed regularly. Determination of trace elements using the Perkin Elmer Elan. The ICP-MS 9000 method was performed with increased precision

and an accuracy exceeding 10% for most elements.

2.4. Data Analysis

Geochemical data are used to determine chemical indices in order to better understand and quantify weathering processes. Two chemical indices were calculated; the Chemical Index of Alteration (CIA) and the Mineralogical Index of Alteration (MIA) according to [23]. These indices are expressed as molecular ratios between mobile and immobile elements and are therefore suitable for defining the intensity of alteration. The CIA evaluates the mobility of cations (Ca^{2+}, Na^{+}, and K^{+}) relative to Al^{3+}, which is considered an immobile element. The MIA determines the degree of transformation of primary minerals into secondary minerals [24]. According to this approach,

$\mathrm{CIA} = \dfrac{\mathrm{Al_2O_3}}{\mathrm{Al_2O_3} + \mathrm{CaO^*} + \mathrm{Na_2O} + \mathrm{K_2O}} \times 100$, (in molar proportion). The MIA is derived from the CIA formula as follows: $\mathrm{MIA} = 2(\mathrm{CIA} - 50)$. The obtained data were processed using the Excel program to generate graphs. The various diagrams were created using Excel and Origin 2018, while the different maps were generated using GOOGLE MAPS, Argis 10.3.1 and QGIS version 2.18.15.

3. Results

3.1. Morphology of the Studied Formations

Morphological characterization distinguished duricrusts that developed on granite from those developed on gneiss, based on altitude, facies and parent rocks (**Figure 4**). These formations outcropped along toposequence with altitudes ranging from 1000 to 1100 m on granite (**Figure 4(a)**) and from 1100 to 1150 m on gneiss (**Figure 4(b)**).

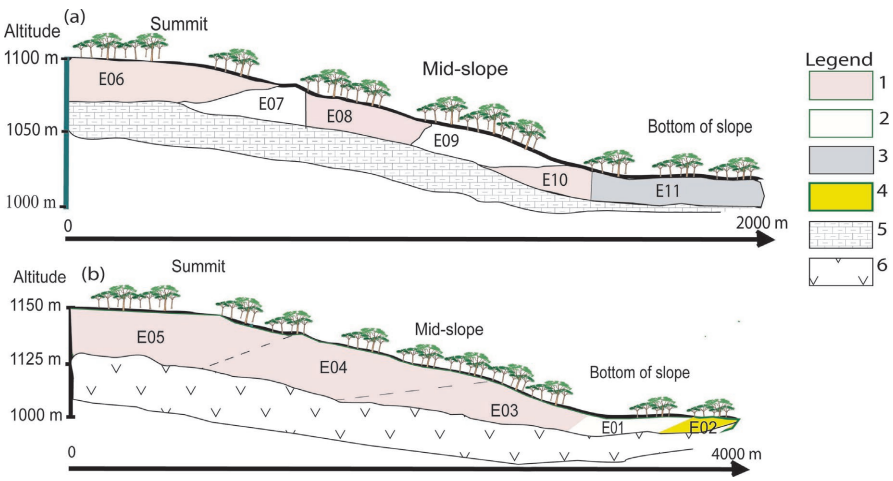

Figure 4. Distribution of different facies of duricrusts along toposequence (1) Massive facies; (2) Nodular facies; (3) Brecciated facies; (4) Vacuolar facies; (5) Gneissic parent rock; (6) Granitic parent rock; (a) duricrusts developed on granite landscape; (b) duricrusts developed on gneiss landscape.

3.1.1. Morphological Characterization of Duricrusts Developed on Granite

The duricrusts found in this area mostly appeared as balls and slabs. Six samples were collected and grouped into three facies: nodular, massive, and vacuolar (**Figure 5**). Nodular facies were more exposed at the top of the hill, less frequently at mid slope, and completely disappeared at the bottom of the slope. Two samples characterized them: the E07 sample collected at the top of the hill (**Figure (5b)**) and the E09 sampled at the mid slope (**Figure 5(d)**). They were both characterized by a yellowish background (5YR5/6) with the cortex slightly altered and containing centimeter-sized nodules heterogeneously distributed. The E07 sample revealed small fragments that scintillate when exposed to sunlight on the matrix background when broken. In contrast to the upper facies (E07), whom matrix showed some traces of biological activity, the harder and more compact mid-slope duricrust (E09), does not contain any traces of biological activity. As for massive duricrust, it was more frequent at the top of the hill (**Figure 5(a)**, **Figure 5(c)**), but also at mid-slope (**Figure 5(e)**). Three samples distinguished them, one at the top (E06) and two at mid-slope (E08 and E10). These materials were all characterized by the tubules that appear as galleries within their matrices. The sample from the top (E06) was very compact and hard, and showed no signs of biological activity (**Figure 5(a)**). In contrast, sample E08 from the mid-slope was less compact and contained an abundance of yellowish spots within the matrix, as well as cavities backfilled with light-dark fine soil, indicating the presence of biological activity. The second mid-slope sample (E10) is distinguished by small spherical concretions relatively uniform in size, ranging from 1 to 5 mm in diameter (**Figure 5(e)**). The vacuolar facies identified by sample E11 (**Figure 5(f)**) was mainly found at the bottom of the slope. They displayed a purplish cortex, a red background (2.5YR4/6) and a large number of intersecting millimeters to centimeters long tubular vacuoles, most of which are filled with reddish fine soil. Biological activity was well developed within them. The matrix also revealed purple bands, whitish and yellowish spots, and lots of small millimeter-sized fragments of quartz and feldspar.

3.1.2. Morphological Characterization of Duricrusts Developed on Gneiss

The duricrusts developed on gneiss outcroped in decimetric and metric blocks. Five samples were collected, two at the top (E04 and E05), one at mid-slope (E03), and two at the bottom (E01 and E02). Their morphological description classified them into three facies: massive, nodular, and brecciated (**Figure 6**). The massive duricrusts were distinguished by three samples (E03, E04, and E05), two collected at the top of the hill (E04, E05) and one at mid-slope (E03). These massive duricrusts were more distributed at the top than mid-slope and completely disappeared at the bottom of the hill. Sample E05, which was very compact and hard, had a dark red background (10R5/3) with reddish, yellowish, and whitish spots. The cortex was purplish and crossed by rare small flutes, indicating biological

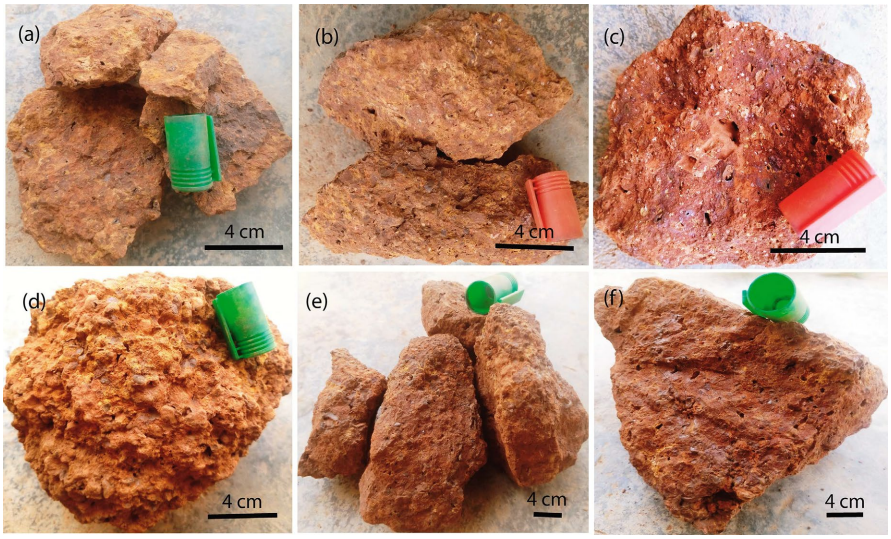

Figure 5. Different facies of duricrust developed on granitic rocks: (a), (c), (e) Massive; (b), (d) Nodular; (f) Vacuolar.

activity. This sample can be qualified as a dark massive duricrust with a purplish area (**Figure 6(a)**). The second sample taken at the top (E04) had a very dark red background (2.5YR2.5/2) and was very compact and hard. It had a dense massive structure. We note the presence of elements that scintillate under sunlight within a microporous matrix with a few rare reddish spots. This sample can be qualified as a dark microporous massive duricrust (**Figure 6(b)**). The third sample (E03), picked up at mid-slope, shows a dark reddish-brown matrix (2.5YR3/4), with a massive and less compact structure. The description revealed the presence of rare flutes, a few whitish and yellowish spots associated with small fragments of quartz (**Figure 6(c)**). Nodular and brecciated duricrusts were mainly found at the bottom of slopes. They were each represented by one sample: E01 for nodular and E02 for brecciated. Nodular duricrusts (**Figure 6(d)**) were characterized by a dark red background (7.5R3/2), containing millimeter to centimeter sized nodules enclosed in very hard and compact cement. The matrix showed yellowish spots and tubules filled with blackish earth. Brecciated formations (**Figure 6(e)**), on the other hand, were characterized by compact blocks whose matrix contained centimeter-sized fragments encased in compact cement. These materials had a dark brown matrix (7.5YR5/8) with centimeter-sized nodules heterogeneously distributed and a few tubules showing signs of biological activity.

3.2. Mineralogical Characterization

In terms of mineralogy, the studied formations were mainly constituted of goethite, hematite gibbsite, kaolinite, and quartz in variable proportions (**Table 1**).

3.2.1. Mineralogy of Duricrusts Developed on Granite

The mineralogical changes observed throughout the three facies (massive, nodular and vacuolar) that characterize this area revealed that mineral proportions varied from one facies to another. Hematite was the most important mineral

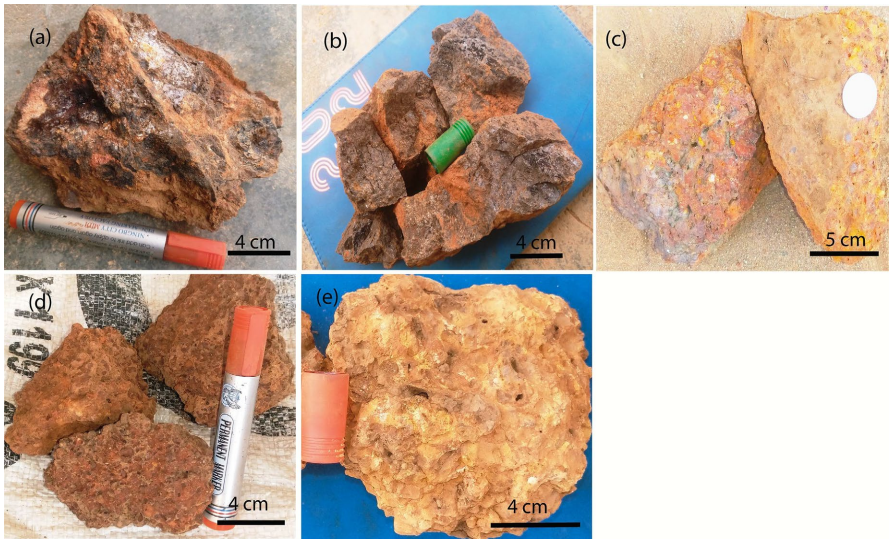

Figure 6. Different facies of duricrust developed on gneissic rocks (a), (b), (c) Massive; (d) Nodular; (e) brecciated.

Table 1. Mineralogical composition of the studied formations (%).

Sectors	Granitic formations (1000 - 1100 m of altitude)						Gneissic formations (1100 - 1150 m of altitude)				
Facies	Massive			Nodular		Vacuolar	Massive			Nodular	Brecciated
Samples	E06	E08	E10	E07	E09	E11	E05	E04	E03	E01	E02
Kaolinite	13.84	9.27	7.31	8.06	13.04	4.12	21.78	9.43	8.21	13.89	22.22
Quartz	6.1	29.11	8.13	27.5	8.5	18.55	-	30.19	18.4	9.71	22.23
Goethite	6.15	11.93	29.27	11.24	21.73	16.5	63.37	30.19	13.7	22.22	11.12
Hematite	46.16	33.77	34.98	26.9	39.13	46.4	11.88	9.43	17.8	38.89	20.51
Gibbsite	27.7	15.9	20.32	26.5	17.4	14.12	2.98	18.85	41.79	15.28	23.93
Total	99.95	99.98	100.01	100.2	99.8	99.69	100.01	98.09	99.9	99.99	100.01

observed in the massive duricrusts. It showed a higher content in the summit formations (E06: 46.16%), followed by those at mid-slope (E08: 33.77%). The most significant quartz, goethite, and gibbsite contents were respectively recorded in E08 (29.13%), E10 (29.27%), and E06 (27.7%) samples. Kaolinite, in contrast, was low in all samples. It ranged from 7.31% in the massive mid-slope duricrusts (E10) to 13.84% for those found at the summit (E06). Concerning nodular duricrusts, the two facies that characterize them (E07 and E09) were mainly composed of hematite, gibbsite, and quartz. Hematite reached a maximum of 39.13% in sample E09 and a minimum of 26.90% in sample E07. Gibbsite and quartz showed high concentrations in the summit formations (E07), with 27.30% for gibbsite and 26.50% for quartz respectively. Kaolinite was poorly distributed within these formations. The vacuolar duricrusts of only one sample (E11) presented the highest hematite content (49.40%) among all the samples from the study area. As showing in Table 1, other minerals such as kaolinite (4.12%), quartz (18.55%), goethite

(16.50%), and gibbsite (14.12%), appeared at relatively lower levels. Figure 7 depicted diffractograms of the identified minerals within granitic formations.

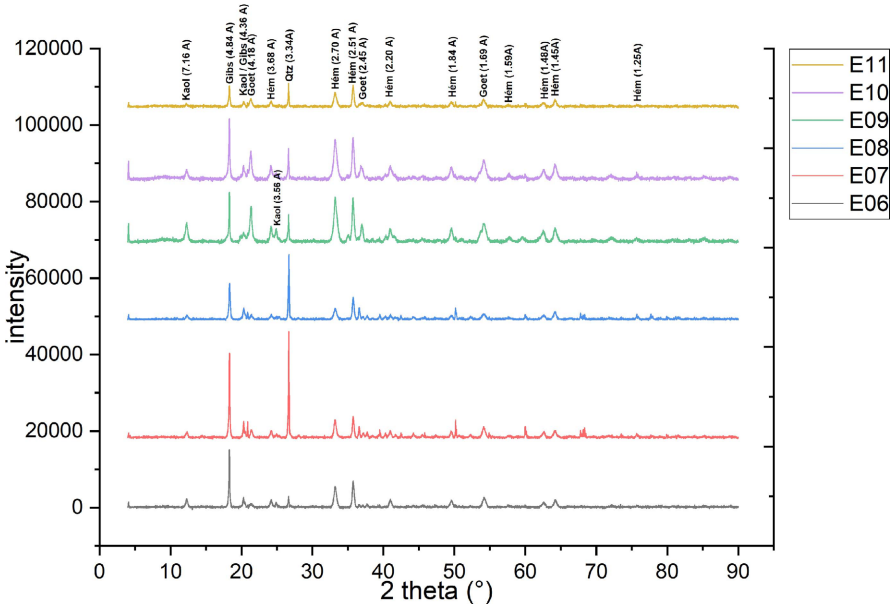

Figure 7. XRD patterns of duricrusts developed on granite.

3.2.2. Mineralogy of Duricrusts Developed on Gneiss

In this area, three facies of duricrusts were found: massive, nodular, and brecciated. The mineralogical assays (Table 1) showed that they were made of goethite, gibbsite, hematite, and kaolinite in variable proportions. The massive duricrusts were distinguished on three samples: E05, E04 and E03. They mainly consisted of goethite, quartz, and gibbsite. Kaolinite and hematite were present in low proportions (Table 1). Goethite had the highest concentration in E05 sample (63.37%) and the lowest in E03 (13.70%). However, gibbsite progressed inversely to goethite, with the highest concentration observed at mid-slope (E03: 41.79%) and the lowest at the top (E05: 2.97%). Quartz reached 30.19% in facies E04 and was not found in facies E05. Nodular duricrust was characterized by E01 sample found at the bottom of the hill. It mainly consisted of hematite (38.89%), followed by goethite (15.28%) and kaolinite (13.89%). Quartz was present at lower proportions (9.72%). The brecciated duricrusts (E02) found at the bottom of the slope displayed moderate contents of kaolinite (22.22%), quartz (22.22%), hematite (20.51%) and gibbsite (23.93%). Goethite was less prevalent (11.12%). Figure 8 depicted diffractograms of the identified minerals within gneissic duricrusts.

3.3. Geochemical Investigations

The geochemistry of investigated formations highlighted major, trace and rare earth elements. Overall, the findings (Table 2) revealed two main groups of major elements based on their concentration throughout the formations. The first group, qualified as the most abundant elements, consisting of Fe_2O_3, Al_2O_3, SiO_2,

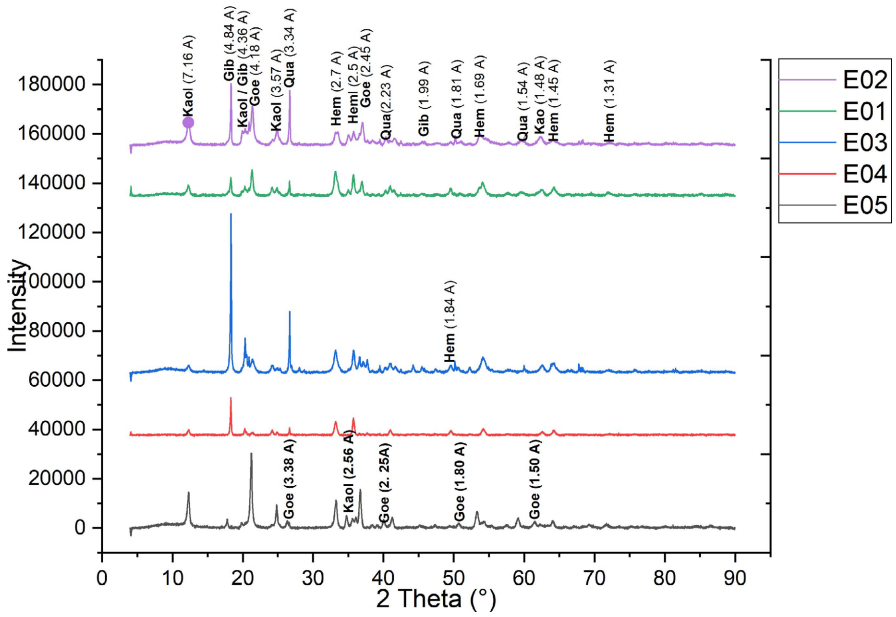

Figure 8. XRD patterns of duricrust developed on gneiss.

and TiO_2, with relatively high concentrations, and a second group composed of alkali metals, alkaline earth metals, and phosphorus, manganese, and chromium oxides (MgO, CaO, Na_2O, K_2O, P_2O_5, MnO, Cr_2O_3), which were found in low proportions. Trace elements (**Table 3**) were characterized by their low concentrations within the formations, except for V, Zr, and Zn, which occur in more significant proportions. **Table 4** and **Table 5** respectively showed rare earth elements and chondrite-normalized rare earth elements of the studied materials. According to these results, light rare earth elements (LREE) are more concentrated than heavy rare earth elements (HREE).

Table 2. Major elements analysis of the studied formations (wt.%), detection limit (DL) = 0.01.

Sectors	Granitic formations (1000 - 1100 m of altitude)						Gneissic formations (1100 - 1150 m of altitude)				
Facies	Massive			Nodular		Vacuolar	Massive		Nodular		Brecciated
Samples	E06	E08	E10	E07	E09	E11	E05	E04	E03	E01	E02
SiO_2	9.78	20.38	9.32	22.48	15.44	9.31	0.95	11.88	13.96	13.46	27.21
Al_2O_3	25.02	26.08	23.31	25.67	20.71	20.57	3.06	10.83	32.36	22.15	26.46
Fe_2O_3	47.88	34.64	49.11	34	49.2	52.93	78.79	63.38	31.85	46.96	28.62
MgO	0.03	0.03	0.04	0.03	0.03	0.02	0.02	0.01	0.04	0.03	0.04
CaO	0.01	0.01	0.04	0.01	0.02	0.01	0.04	0.01	0.04	0.02	0.03
Na_2O	0.01	0.01	0.01	0.01	0.01	0.01	0.01	0.01	0.01	0.01	0.01
K_2O	0.01	0.04	0.01	0.03	0.01	0.01	0.01	0.01	0.05	0.04	0.08
TiO_2	1.23	1.47	1.35	1.12	0.94	1.15	0.52	0.47	1.16	0.92	0.78
P_2O_5	0.3	0.07	0.21	0.21	0.18	0.17	2.97	0.9	0.38	0.47	0.28
MnO	0.03	0.03	0.04	0.02	0.03	0.02	0.26	0.25	0.03	0.03	0.03

Continued

Cr_2O_3	0.103	0.05	0.07	0.069	0.155	0.071	0.031	0.007	0.089	0.172	0.09
LOI	15.3	17	16.2	16.2	13	15.4	13	12.1	19.8	15.4	16.1
Total	99.69	99.76	99.71	99.79	99.7	99.68	99.79	99.87	99.72	99.68	99.75
CIA	99.88	99.73	99.57	99.77	99.71	99.81	96.84	99.63	99.57	99.60	99.44
MIA	99.68	99.46	99.15	99.53	99.42	99.61	93.67	99.26	99.14	99.19	98.87

Table 3. Trace elements content (ppm).

Sectors	Traces elements of duricrusts developed on granite						Traces elements of duricrusts developed on gneiss				
Facies	Massive			Nodular		Vacuolar	Massive		Nodular		Brecciated
Samples	E06	E08	E10	E07	E09	E11	E04	E05	E03	E01	E02
Ba	22	17	18	21	15	14	1191	476	61	135	5
Co	4.2	5.2	4	3.8	5.4	4.5	91.6	28.4	6.6	4.7	5.6
Cs	0.2	0.5	0.1	0.2	0.1	0.2	0.1	0.1	0.3	0.3	0.4
Cu	34.6	48.8	31.9	26.7	62.5	41.6	143.9	111.6	16.6	38.4	59.9
Ga	41.2	45	42.8	31.6	38.6	43.3	3.6	13.8	41.1	42.4	37.1
Hf	8.1	12.2	11.2	10.5	10.4	9.8	0.2	3.7	12.5	9.9	10.2
Mo	8.8	5.2	8.6	5.2	6.9	8.7	8.4	0.5	7.3	4.8	7.9
Nb	20.3	25.7	22.9	19.1	15.4	21.1	2.5	8.8	23.4	14.7	17.7
Ni	13.2	11.1	11.4	12.5	15.5	14.6	294.8	165	13.4	16	18.2
Pb	33.7	40.1	38	29	38.7	41.4	1.4	60.6	22.3	13.8	23.3
Rb	1.8	3.8	1.4	3.5	2.2	1.8	0.2	0.8	4.2	7.7	3.9
Sb	0.6	0.4	0.7	0.4	0.4	0.6	0.1	0.1	0.8	0.1	0.4
Sc	34	38	34	24	34	35	13	22	21	36	34
Sn	8	6	2	4	3	7	1	1	6	3	3
Sr	12.2	7	10	10.5	7.3	5.5	140.9	1.1	27.5	44.6	58.5
Th	23.3	30.5	18.9	27.8	25.5	16.8	0.9	3.6	14.4	10.8	17.9
U	8.4	12.8	8.5	12.5	4.8	8	0.6	3	6.1	7	5.1
V	1079	614	978	540	1005	1118	255	108	851	690	1016
W	2.8	1.7	1.7	1.2	1.4	2.4	0.5	0.5	2.5	3.1	1.8
Y	8.1	9.6	7.9	7.6	5.5	8.8	13.1	15	10.7	9.7	11.8
Zn	9	3	6	7	19	6	552	259	5	31	26
Zr	323.6	493.8	467.4	406.7	432.1	401	9.6	145.4	520.4	409.7	425.4

Table 4. Rare earth elements content (ppm).

Sectors	Granitic formations (1000 - 1100 m of altitude)						Gneissic formations (1100 - 1150 m of altitude)				
Facies	Massive			Nodular		Vacuolar	Massive			Nodular	Brecciated
Samples	E06	E08	E10	E07	E09	E11	E04	E05	E03	E01	E02
Altitude (m)	1090	1070	1020	1050	1040	1000	1140	1130	1120	1110	1100

Continued

La	20.7	13.4	15.8	17.3	12	12	6.3	34.6	27.3	42.2	39.8
Ce	47.4	54	57.6	37.1	29.3	42.3	115.3	79.9	48	74.9	76.9
Pr	4.01	2.85	3.28	3.13	2.31	3.07	1.62	8.87	5.19	8.14	8.68
Nd	14	10.1	11.7	10.5	8.2	11.5	6	33.7	18.1	28.4	31.7
Sm	2.68	1.98	2.25	2.14	1.64	2.53	1.56	6.49	3.18	4.83	5.65
Eu	0.6	0.41	0.5	0.41	0.37	0.51	0.44	1.61	0.71	1.08	1.3
Gd	2.03	1.75	1.79	1.73	1.25	1.94	2.06	4.85	2.57	3.52	4.13
Tb	0.3	0.29	0.3	0.29	0.21	0.33	0.4	0.58	0.38	0.47	0.53
Dy	1.77	1.8	1.76	1.73	1.25	1.93	3.3	2.83	2.22	2.56	2.82
Ho	0.34	0.37	0.35	0.33	0.25	0.37	0.74	0.49	0.42	0.45	0.52
Er	1	1.17	1.02	1.05	0.75	1.14	2.82	1.29	1.22	1.26	1.43
Tm	0.15	0.18	0.16	0.17	0.11	0.19	0.47	0.16	0.19	0.17	0.21
Yb	1.05	1.3	1.17	1.18	0.84	1.35	3.64	0.95	1.38	1.17	1.39
Lu	0.16	0.2	0.17	0.17	0.12	0.18	0.56	0.14	0.2	0.18	0.19
REE	96.19	89.8	97.85	77.23	58.6	79.34	145.21	176.46	111.06	169.33	175.25
LREE	89.39	82.74	91.13	70.58	53.82	71.91	131.22	165.17	102.48	159.55	164.03
HREE	6.8	7.06	6.72	6.65	4.78	7.43	13.99	11.29	8.58	9.78	11.22

Table 5. Chondrite-normalized rare earth elements content (ppm).

Sectors	Gneissic formations (1000 - 1100 m of altitude)					Granitic formations (1100 - 1150 m of altitude)					
Samples	E01	E02	E03	E04	E05	E06	E07	E08	E09	E10	E11
La	42.20	39.80	27.30	34.60	6.30	20.70	17.30	13.40	12.00	15.80	12.00
Ce	25.19	25.87	16.15	26.88	38.78	15.94	12.48	18.16	9.86	19.37	14.23
Pr	19.91	21.23	12.70	21.70	3.96	9.81	7.66	6.97	5.65	8.02	7.51
Nd	14.73	16.44	9.39	17.48	3.11	7.26	5.45	5.24	4.25	6.07	5.96
Sm	7.20	8.43	4.74	9.68	2.33	4.00	3.19	2.95	2.45	3.36	3.77
Eu	4.42	5.32	2.91	6.59	1.80	2.46	1.68	1.68	1.52	2.05	2.09
Gd	3.51	4.12	2.56	4.84	2.05	2.02	1.72	1.74	1.25	1.78	1.93
Tb	2.95	3.32	2.38	3.64	2.51	1.88	1.82	1.82	1.32	1.88	2.07
Dy	2.53	2.78	2.19	2.79	3.26	1.75	1.71	1.78	1.23	1.74	1.91
Ho	1.86	2.15	1.74	2.03	3.07	1.41	1.37	1.53	1.04	1.45	1.53
Er	1.77	2.01	1.72	1.82	3.97	1.41	1.48	1.65	1.06	1.44	1.61
Tm	1.56	1.93	1.74	1.47	4.31	1.38	1.56	1.65	1.01	1.47	1.74
Yb	1.92	2.29	2.27	1.56	5.99	1.73	1.94	2.14	1.38	1.92	2.22
Lu	1.68	1.78	1.87	1.31	5.23	1.50	1.59	1.87	1.12	1.59	1.68

The chondrite-normalized rare earth elements patterns generally reveal slight positive Ce and Yb anomalies. Ce anomaly is more significant in Sample E05, the massive duricrust developed on gneiss (Figure 9(a)).

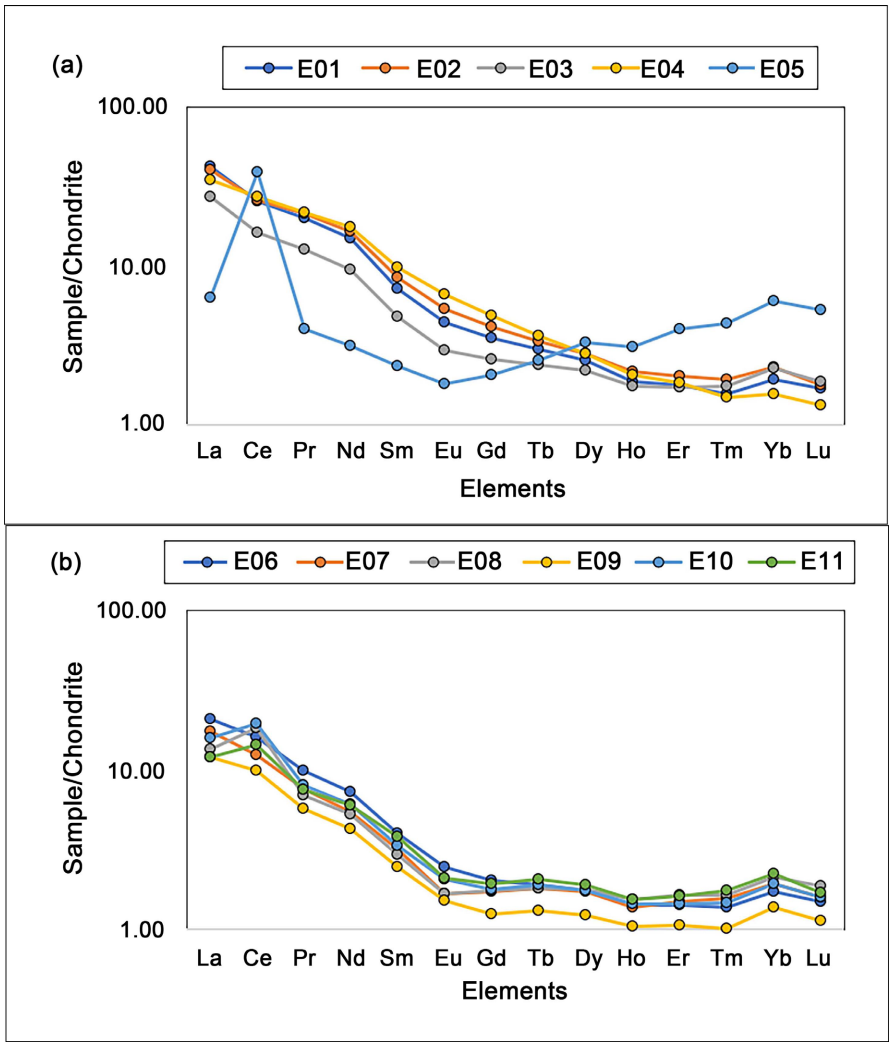

Figure 9. Chondrite-normalized rare earth elements patterns within studied formations: (a) gneissic formations, (b) granitic formations.

3.3.1. Geochemistry of Duricrusts Developed on Granite

In duricrusts formed on granite, the two main oxides (Fe_2O_3 and Al_2O_3) were distinguished by opposite trends in the various facies, with Fe_2O_3 concentrations decreasing and Al_2O_3 increasing when altitude increases. Thus, massive duricrust was marked by an Fe_2O_3 content of 47.88% at the summit (E06) and 49.2% at mid-slope (E10). Similarly, nodular duricrust revealed Fe_2O_3 proportions of 34% at the summit (E07) compared to 49.2% at mid-slope (E09). The highest Fe_2O_3 content (52.93%) was found in vacuolar facies (E11), outcropping at the bottom of slopes (1100 m). Al_2O_3 was distinguished by its opposite pattern, increasing with altitude. Thus, in massive duricrusts, we observed values of 20.71% in sample E10 from the mid-slope, which are much lower than those found in sample E06 (25.02%) from

the summit. Similarly, nodular duricrusts from the mid-slope were characterized by a lower Al_2O_3 content (20.71%) than those from the summit (25.67%). The lowest Al_2O_3 content (20.57%) was observed in vacuolar facies (E11) found at the bottom of hill. SiO_2 contents varied from 9.32% in massive mid-slope facies to 22.48% in those found at the top. It ranged from 15.44% for mid-slope formations to 22.48% for those at the top in nodular formations. It was 9.31% in the vacuolar duricrusts at the bottom of slopes. TiO_2 was lower. Its content varied from 0.94% to 1.35%.

Alkaline and alkaline earth metals, as well as phosphorus, manganese, and chromium oxides, appeared in very low proportions (average sum < 1%). Trace elements were mainly constituted by V and Zr, whose proportions differ from one facies to another. In massive crusts, V ranged from 978 to 1079 ppm and Zr from 323.6 to 467.4 ppm. In nodular crusts, V was between 540 and 614 ppm and Zr between 406.7 and 493.8 ppm. Vacuolar duricrusts had a V content of 1118 ppm and a Zr content of 401 ppm. Light rare earth elements were distinguished by higher contents than heavy rare earth elements (**Table 4**). The sum of light rare earth elements within duricrusts developed on granite was 459.57 ppm, while that of heavy rare earth elements was 39.44 ppm.

3.3.2. Geochemistry of Duricrusts Developed on Gneiss

The duricrusts developed on gneiss displayed an opposite behavior in terms of the evolution of the two major oxides (Fe_2O_3 and Al_2O_3). While Fe_2O_3 increased with altitude, Al_2O_3 tends to decrease. This trend was observed in massive duricrusts, which had a higher Fe_2O_3 content (78.79%) in sample E05 from the summit (1150 m) and a lower content (31.85%) in sample E03 from mid-slope (1120 m). At the intermediate level (1130 m), this content was 63.38%. The nodular duricrusts found at the bottom of slope (1110 m) revealed a relatively high Fe_2O_3 content (46.96%), while the brecciated duricrusts also found at the bottom of slope (1100 m) contained the lowest Fe_2O_3 concentrations (28.62%). SiO_2 followed the same trend as Al_2O_3. It appeared at low concentration in the massive duricrust at the summit (E05: 0.95%) and relatively high in samples E04 (13.96%) and E03 (11.88%) from the mid-slope. This content was 13.46% in nodular duricrust and 27.21% in brecciated, both outcropping at the bottom of slopes. Overall, TiO_2 content was less than 1% in all samples except for E03 (1.16%).

Alkaline and alkaline earth metals, phosphorus, manganese, and chromium oxides, were found in very low proportions (sum of averages < 1%). In massive armor, trace elements were mainly represented by Ba (61-1191 ppm), V (108 - 851 ppm), Zn (5 - 259 ppm), Ni (13.4 - 294.8 ppm), Cu (16.6 - 143.9 ppm) and Sr (1.1 - 140.9 ppm). In nodular formations, we noted V (690 ppm), Zr (409.7 ppm) and Ba (135 ppm) as the most abundant trace elements, while in brecciated duricrusts, they were V (1016 ppm) and Zr (425.4 ppm).

Light rare earth elements were more concentrated than heavy rare earth elements in all samples from this study area (**Table 4**). The sum of light rare earth elements was 722.45 ppm, while that of heavy rare earth elements was 54.86 ppm.

3.3.3. Evolution of Two Main Oxides within the Studied Formations

Geochemical concentrations of the two main oxides (Al_2O_3 and Fe_2O_3) within duricrust formations on the two parent rocks indicate opposite trends. While Al_2O_3 increases with altitude on granite formations and Fe_2O_3 decreases, it decreases on gneiss formations and Fe_2O_3 increases (Figure 10).

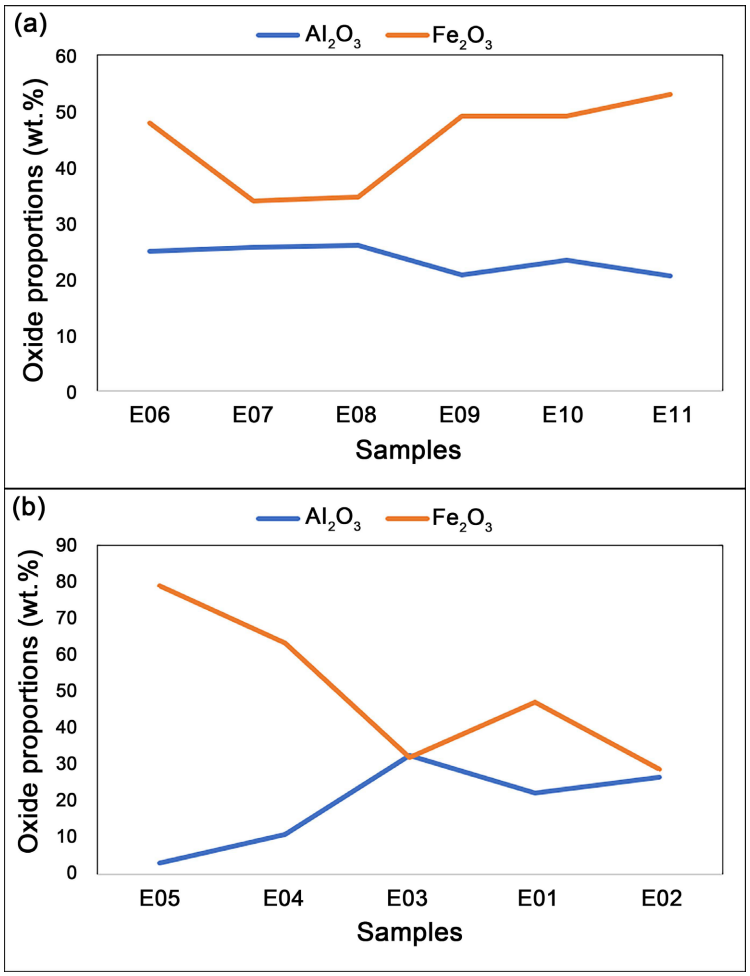

Figure 10. Opposite evolution of iron and aluminum oxides within studied duricrusts: (a) granitic sector, (b) gneissic sector.

4. Discussion

4.1. Morphological, Mineralogical and Toposequential Transformations of the Studied Duricrusts

Intertropical areas characterized by contrasted climate, promote the development of duricrusts and several facies are most frequently identified [1]. These involve specific processes and environmental conditions that prevailed during their genesis, relating to various phases of weathering [2] [25]. Their evolution supports the fact that they derive from the erosion and sedimentation of older formations, and possibly from eroded forms that developed over the exposed platforms [26].

Four facies are found in the studied area: massive, nodular, vacuolar and brecciated. They have been developed with the influence of biological activities, including roots, microorganisms, and soil fauna which play an important role in shaping the microstructure and facies of duricrusts [27]. Indeed, these activities often create features such as tubules and vacuoles that influence porosity, mineral precipitation, and element mobility [26]. In addition, depending on the intensity and type of bioturbation, soil fauna (termites) mixes materials vertically and laterally, disrupting stratification and creating diverse facies (nodular, pisolitic, or massive). This has been demonstrated by [28] who noted in their work that the intensity and nature of biological activities directly influence the morphology of duricrusts developed. Massive facies represent a mature duricrust and suggest low permeability, stable conditions, and minimal reworking [29]. Nodular facies composed of discrete iron-rich nodules, reflect partial degradation of massive duricrust [30] [31] whereas vacuolar facies for its part, contain voids or cavities, often irregular and interconnected suggesting dissolution of soluble components during hardening [29] [32]. The brecciated facies reflect a late transformation, probably linked to landscape instability or [30].

The toposequential trends indicate hilltops with more evolved duricrusts, thick and more altered than on lower slopes as highlighted by [14], in their work on the influence of topography in duricrust development in the Ngaoundal-Dir section of central Cameroon. Similar works have been conducted on the lateritic landforms of the Bamileke plateau, where two distinct landforms were identified, with one more mature than the other [8]. Thus, altitude plays an important role in the processes shaping the development of duricrusts [33].

Table 1 shows relatively high iron oxides, notably hematite in massive, nodular, and vacuolar crusts on granite (26.9% to 46.4%) and goethite in nodular crusts on gneiss (30.19 to 63.37). These findings are probably due to ferruginization, a pedogenic and geochemical process through which iron oxides (mainly Fe^{3+} in the form of goethite and hematite) accumulate in soils or weathering profiles to form ferruginous duricrusts [34] [35]. The low kaolinite values recorded in the granitic formations (4.12 to 14.84%) and the relatively higher values in the gneissic (8.21 to 22.22%) attest to a moderate process of monosillitization. This refers to the transformation of primary minerals (such as feldspars) into base-poor clays, particularly kaolinite, under the action of water and environmental acidity [1] [34]. The varying proportions of gibbsite in certain facies within the studied formations, reaching up to 41.79% in massive duricrusts developed on gneiss, combined with hematite and goethite content (**Table 1**), would reflect the process of allitization under conditions of intense weathering in a hot, humid climate with high rainfall [1] [34].

The high CIA and MIA values (>99), combined with low alkali and alkaline earth metal values, clearly confirm intense weathering processes along topographic sequences during the pedogenic processes that prevailed during the development of the studied duricrusts [23] [36] [37].

4.2. Evolution of Major Oxides within Duricrusts Developed on Granitic and Gneissic Rocks

Duricrusts developed on granite indicate higher concentration of aluminum at high altitudes, compared to iron, which is more concentrated at lower altitudes. This would indicate acidic and well-drained conditions that favored the mobility of iron as Fe^{2+}. Indeed, high altitudes provide better drainage, promoting iron leaching and residual aluminum concentration. At low altitudes, iron precipitates as hematite or goethite under more humid and reducing conditions [14] [32] [38]. In addition, the alteration of feldspars from granitic rocks leads to the release of aluminum, which can concentrate as gibbsite within the intermediate zones, and thus displace iron, which is most susceptible to mobility towards the lower areas [39]. Thus, the results display vertical organization of the studied materials with iron-rich duricrusts at the top, bauxitic crusts at mid-slope, and kaolinitic levels at the bottom of the slope, corresponding to the toposequential models described by [2] in Haut-Katanga, where topography controls the processes of weathering, drainage, and elements concentration. Similar studies have been conducted in Cameroon in Mandjou, Eastern Cameroon, by [40], where differentiation of lateritic crusts on granite substrates was observed according to landscape position.

The duricrusts developed on gneiss displays the opposite pattern. These contain more iron at high altitudes and aluminum at low altitudes. This contrasting evolution of aluminum and iron within these formations, is probably due to differences in mineralogy, weathering conditions, and the hydrological dynamics of the parent rocks. In general, granite is rich in feldspars, particularly plagioclases and K-feldspars. Their alteration leads to the formation of aluminous minerals such as kaolinite and gibbsite. Gneiss, though also feldspathic, often contains more biotite and other ferromagnesian minerals, which are richer in iron. This trend reduces the initial source of aluminum at high altitudes within gneissic formations as in the specific case of the E05 sample (3.06%) [41]. On granite, weathering at high altitudes presents better drainage and leaching conditions, favoring the removal of mobile elements (Na, K, Ca), leaving behind residual Al in the form of gibbsite [42]. On gneiss, the breakdown of Fe-rich minerals at high altitudes may lead to iron accumulation due to less intense leaching or different redox conditions [31].

Furthermore, at high altitudes, conditions are often colder, more acidic, and less humid than in lower areas, promoting the release of aluminum as soluble complexes and the residual accumulation of iron, notably as hematite or goethite [43]. Elevated areas are often well drained, favoring iron oxidation and precipitation as Fe_2O_3. Aluminum, which is more mobile under these conditions, is leached to lower levels or exported from the system [44]. It has been demonstrated that the presence of gibbsite in the intermediate levels suggests a high mobilization of aluminum, while the dominance of hematite at the top reflects a residual concentration of iron [32] [38]. All of these studies clearly highlight various dynamics of duricrust landscapes overall, but particularly within the inter-tropical zone.

4.3. Trace Element Enrichment and Anomaly Analysis

The relative high concentrations of certain trace elements including V, Zr, Cr and Ba in the studied formations can be explained through a combination of geochemical and environmental processes. Indeed, tropical weathering removes mobile elements (Mg, Ca, Na), contributing to the accumulation of less mobile elements like Cr, Zr and V and enrichment of secondary mineral like hematite, goethite and kaolinite [31]. Environmental and geological controls also play an important role in these processes. Whereas alternating wet and dry seasons promote dissolution and precipitation of elements, weathering of rich underlying rocks can concentrate elements as so as gently sloping areas to favor duricrust formations and element accumulation [14] [45].

It is demonstrated that positive Ce anomalies in lateritic formations are mineralogically related to the precipitation of cerianite (CeO_2) due to the Ce^{3+} to Ce^{4+} redox change [46] [47]. Positive Yb anomalies may result from differential mobility of rare earth elements during intense weathering inducing relative enrichment of Yb, particularly where light rare earth elements are leached more easily [48] [49]. Yb forms stable complexes in acidic condition favoring its retention [50].

5. Conclusions

The study permitted to characterize duricrusts from Meiganga, grouped into four main facies: massive and nodular facies found at both sites, vacuolar exclusively on granitic rocks between 1000 and 1100 m of altitude and brecciated facies on gneissic rocks with altitude 1100 to 1150 m. The study results revealed that the toposequential evolution of these formations, displays an interaction between various parameters such as lithology, geomorphology and pedogenic processes that favored their establishment. The vertical differentiation in mineral compositions, characterized by aluminum-rich zones, dominated by gibbsite and iron-rich domains, characterized by hematite and goethite, reflects the influence of altitude, drainage, and bedrock composition on the development of these lateritic formations. Granitic environments tend to favor aluminum enrichment at high altitudes and iron concentration at low altitudes, due to feldspar weathering and well-drained conditions, while gneissic areas favor iron accumulation through the weathering of ferromagnesian minerals.

This study significantly contributes to the understanding of the mechanisms involved in the lateritic formations within tropical environments by highlighting the influence of topographic gradients and lithological contrasts that govern the geochemical distribution of chemical elements. This insight is essential for interpreting the evolution of intertropical duricrust landscapes in general and those of Adamawa in particular.

Conflicts of Interest

The authors declare no conflicts of interest regarding the publication of this paper.

References

[1] Tardy, Y. (1993) Pédologie des latérites et des sols tropicaux. Masson, 459 p.

[2] Alexandre, J. (2002) Les cuirasses latéritiques et autres formations ferrugineuses tropicales: Exemple du Haut-Katanga méridional. *Annales—Sciences Géologiques*, **107**, p. 119.

[3] Blot, A. (2004) Caractérisation des chapeaux de fer en milieu latéritique cuirassé. *Comptes Rendus. Géoscience*, **336**, 1473-1480. https://doi.org/10.1016/j.crte.2004.07.008

[4] Likiby, B. (2010) Géochimie et géotechnique des formations superficielles de la région de Maroua (Nord-Cameroun): Intérêts environnementaux et industriels, Master's Thesis, Faculté des Sciences—Université de Yaoundé I, 293 p.

[5] Nahon, D., Tardy, Y. and Oliveira, J.M. (1992) Geochemical Evolution of Lateritic Profiles in the Amazon Basin: The Barreiras Croup of Brazil. In: Rose, C.W., Watson, A.J. and Matthews, R.H., Eds., *Weathering, Soils and Paleosols*, Elsevier, 187-204.

[6] Colin, F., Beauvais, A., Ambrosi, J.P. and Nahon, D. (2004) Les latérites en environnement tropical, source de métaux d'intérêt économique. *Assises de la Recherche Française dans le Pacifique*, Nouméa, 24 au 27 août 2004, 103-107. https://horizon.documentation.ird.fr/exl-doc/pleins_textes/divers14-02/010051927.pdf

[7] Letouzey, R. (1979) Végétation du Cameroun. In: Laclavère, G., Ed., *Atlas de la République Unie du Cameroun*, Jeune Afrique, 13-15.

[8] Momo, M.N., Yemefack, M., Tematio, P., Beauvais, A. and Ambrosi, J. (2016) Distribution of Duricrusted Bauxites and Laterites on the Bamiléké Plateau (West Cameroon): Constraints from GIS Mapping and Geochemistry. *CATENA*, **140**, 15-23. https://doi.org/10.1016/j.catena.2016.01.010

[9] Tematio, P., Meli Songmene, S., Leumbe Leumbe, O., Momo Nouazi, M., Yemefack, M. and Yongue-Fouateu, R. (2017) Mapping Bauxite Indices Using Landsat ETM+ Imageries Constrained with Environmental Factors in Foumban Area (West Cameroon). *Journal of African Earth Sciences*, **129**, 806-819.

[10] Zame, P.Z., Assomo, P.S. and Onwualu, J.N. (2017) Assessment of Geotechnical Properties of Lateritic Gravels from South-Cameroon Road Network. *International Journal of Geosciences*, **8**, 949-964. https://doi.org/10.4236/ijg.2017.88054

[11] Sojien, T.M., Mamdem, E.L.T., Wouatong, A.S.L. and Bitom, D.L. (2018) Mineralogical, Geochemical and Distribution Study of Bauxites in the Locality of Bangam and Environs (West Cameroon). *Earth Science Research*, **7**, 117-130. https://doi.org/10.5539/esr.v7n1p117

[12] Ahmadou, A., Ondoa, A.D.B., Sini, A. and Nguetnkam, J.P. (2023) Morphological, Mineralogical and Geochemical Characterization of the Danfili-Mambal Duricrust Formations (Adamawa-Cameroon). *Scientific African*, **21**, e01873. https://doi.org/10.1016/j.sciaf.2023.e01873

[13] Sini, A., Boukari, H., Balla, O.A.D., Beral, D., Awé, S.W., Basga, S.D., *et al.* (2024) Mobility of Major and Trace Elements during the Bauxitization Processes in Ngaoundal Area (Adamawa Cameroon): Implication on Mining Perspectives. *Open Journal of Geology*, **14**, 81-100. https://doi.org/10.4236/ojg.2024.141005

[14] Sini, A., Basga, S.D., Temga, J.P. and Nguetnkam, J.P. (2020) The Influence of Topography in Duricrust Development in the Ngaoundal-Dir Section of Central Cameroon: Understanding Morphological, Mineralogical and Geochemical Transformations. *Scientific African*, **10**, e00655. https://doi.org/10.1016/j.sciaf.2020.e00655

[15] Nguetnkam, J.P. (2004) Les argiles des Vertisols et des sols fersiallitiques de l'Extrême Nord du Cameroun: genèse, propriétés cristallochimiques et texturales, typologie et application à la décoloration des huiles végétales. Thèse de Doctorat d'État, Université de Yaoundé I, 216 p.

[16] WRB (2022) International Soil Classification System for Naming Soils and Creating Legends for Soil Maps. 4th Edition, International Union of Soil Sciences (IUSS).

[17] Yonkeu, S. (1993) Végétation des pâturages de l'Adamaoua (Cameroun): Écologie et potentialités pastorales. Thèse de Doctorat, Université de Rennes I, 213 p.

[18] Tchameni, R., Pouclet, A., Penaye, J., Ganwa, A.A. and Toteu, S.F. (2006) Petrography and Geochemistry of the Ngaoundéré Pan-African Granitoids in Central North Cameroon: Implications for Their Sources and Geological Setting. *Journal of African Earth Sciences*, **44**, 511-529. https://doi.org/10.1016/j.jafrearsci.2005.11.017

[19] Keutchafo Kouamo, N., Tchatptchet, D.T., Tezanou Ngueguim, A.L., Simeni Wambo, N.A., Tchouankoue, J.P. and Cucciniello, C. (2019) Petrogenesis of Basaltic Dikes from the Manjo Area (Western Cameroon): Insights into the Paleozoic Magmatism at the Northern Margin of the Congo Craton in Cameroon. *Arabian Journal of Geosciences*, **12**, Article No. 281. https://doi.org/10.1007/s12517-019-4424-y

[20] Moreau, C., Regnoult, J., Déruelle, B. and Robineau, B. (1987) A New Tectonic Model for the Cameroon Line, Central Africa. *Tectonophysics*, **141**, 317-334. https://doi.org/10.1016/0040-1951(87)90206-x

[21] Ngounouno, I., Moreau, C., Deruelle, B., Demaiffe, D. and Montigny, R. (2001) Petrologie du complexe alcalin sous-sature de Kokoumi (Cameroun). *Bulletin de la Société Géologique de France*, **172**, 675-686. https://doi.org/10.2113/172.6.675

[22] McDonough, W.F. and Sun, S. (1995) The Composition of the Earth. *Chemical Geology*, **120**, 223-253. https://doi.org/10.1016/0009-2541(94)00140-4

[23] Nesbitt, H.W. and Young, G.M. (1982) Early Proterozoic Climates and Plate Motions Inferred from Major Element Chemistry of Lutites. *Nature*, **299**, 715-717. https://doi.org/10.1038/299715a0

[24] Price, J.R. and Velbel, M.A. (2003) Chemical Weathering Indices Applied to Weathering Profiles Developed on Heterogeneous Felsic Metamorphic Parent Rocks. *Chemical Geology*, **202**, 397-416. https://doi.org/10.1016/j.chemgeo.2002.11.001

[25] Martins, R. (2024) Genèse et évolution des cuirasses ferrugineuses dans la for-mation Barreiras, marge sud-est du Brésil. Thèse de doctorat, Sorbonne Université en cotutelle avec Universidade Federal de Ouro Preto, École doctorale Géosciences, ressources naturelles et environnement.

[26] Nouazi Momo, M., Beauvais, A., Tematio, P., Ambrosi, J., Yemefack, M., Yerima, B.P.K., *et al.* (2019) Lateritic Weathering of Trachyte, and Bauxite Formation in West Cameroon: Morphological and Geochemical Evolution. *Journal of Geochemical Exploration*, **205**, Article ID: 106324. https://doi.org/10.1016/j.gexplo.2019.06.006

[27] Boeva, N., Bortnikov, N., Slukin, A., Shipilova, E., Makarova, M. and Melnikov, P. (2021) Biofilms and Biominerals in the Lateritic Weathering Crust as Exemplified by the Central Bauxite Deposit (Siberian Platform, Russia). *Minerals*, **11**, Article 1184. https://doi.org/10.3390/min11111184

[28] Boulange, B., Ambrosi, J. and Nahon, D. (1997) Laterites and Bauxites. In: Boulange, B., Ambrosi, J. and Nahon, D., Eds., *Soils and Sediments*, Springer, 49-65. https://doi.org/10.1007/978-3-642-60525-3_3

[29] Dixon, J.C. and McLaren, S.J. (2009) Duricrusts. In: Parsons, A.J. and Abrahams, A.D., Eds., *Geomorphology of Desert Environments*, Springer, 123-151.

https://doi.org/10.1007/978-1-4020-5719-9_6

[30] Bitom, D. and Volkoff, B. (1993) Altération déferruginisante des cuirasses massives et formation des horizons gravillonnaires ferrugineux dans les sols de l'Afrique Centrale humide. *Comptes Rendus de l'Académie des Sciences de Paris, Série II*, **316**, 1447-1454.

[31] Fenske, C., Braun, J., Guillocheau, F. and Robin, C. (2022) Models of Duricrust Formation in Tropical and Subtropical Areas. *EGU General Assembly* 2022, Vienna, 23-27 May 2022, EGU22-4412. https://doi.org/10.5194/egusphere-egu22-4412

[32] Tardy, Y. (1997) Petrology of Laterites and Tropical Soils. A.A. Balkema.

[33] Fenske, C., Braun, J., Guillocheau, F. and Robin, C. (2023) Comparing Models for Duricrust Formation in Tropical and Subtropical Areas. HAL Open Archive. https://hal.science/hal-04082134

[34] Nahon, D. (1991) Introduction to the Petrology of Soils and Chemical Weathering. John Wiley & Sons, 313 p.

[35] Nguetnkam, J., Villiéras, F., Ekodeck, G.E. and Yvon, J. (2008) Clay Minerals and Geochemistry of Two Lateritic Profiles Developed on Gneiss and Granite in the Humid Tropical Climate of CAMEROON (Central Africa). *Geoderma*, **145**, 351-361.

[36] Babechuk, M.G. and Fedo, C.M. (2023) Analysis of Chemical Weathering Trends across Three Compositional Dimensions: Applications to Modern and Ancient Mafic-Rock Weathering Profiles. *Canadian Journal of Earth Sciences*, **60**, 839-864. https://doi.org/10.1139/cjes-2022-0053

[37] Maslov, A.V. and Podkovyrov, V.N. (2023) Chemical Weathering Indexes: Implication for Paleoclimatic Reconstructions, with the Vendian-Lower Cambrian Section of Podolian Transnistria as Example. *Lithology and Mineral Resources*, **58**, 213-234. https://doi.org/10.1134/s0024490222700043

[38] Beauvais, A. (1991) Formation and Transformation Processes of Iron Duricrust System under Tropical Humid Environment. *EUROLAT'91—Supergene Ore Deposits and Mineral Formation*, 5*th International Meeting*, Berlin, 23-24 August 1991, 34-39.

[39] Nguetnkam, J.P., Yongue-Fouateu, R., Bitom, D., Bilong, P. and Volkoff, B. (2005) Étude pétrologique d'une formation latéritique sur granite en milieu tropical forestier sud-camerounais (Afrique centrale): Mise en évidence de son caractère polyphasé. *Étude et Gestion des Sols*, **13**, 111-126.

[40] Mebouinz, A. and Onana, V.L., (2021) Évolution des cuirasses latéritiques sur substrat granitique dans la région de Mandjou (Est-Cameroun). *Journal Camerounais de Géosciences*, **15**, 45-60.

[41] Bhat, N.A., Ghosh, P., Ahmed, W., Naaz, F. and Darshinee, A.P. (2022) Comparative Evaluation of Weathering Indices of Rock-Soil Sequences in Parts of Peninsular Gneissic Complex, Western Dharwar Craton, Karnataka, India. *Arabian Journal of Geosciences*, **15**, Article No. 1087. https://doi.org/10.1007/s12517-022-09459-8

[42] Boeva, N.M., Makarova, M.A., Shipilova, E.S., Slukin, A.D., Soboleva, S.V., Zhegallo, E.A., *et al.* (2022) Gibbsite and Boehmite in Weathering Crusts of Different Ages Affected by Lateritization: Location and Formation. *Doklady Earth Sciences*, **504**, 353-361. https://doi.org/10.1134/s1028334x22060046

[43] Regmi, A.D., Yoshida, K., Dhital, M.R. and Pradhan, B. (2013) The Relationship between Geology and Rock Weathering on the Rock Instability along Mugling-Narayanghat Road Corridor, Central Nepal Himalaya. *Environmental Earth Sciences*, **70**, 3069-3081.

[44] Souaibou, F., Nguetnkam, J.P., Bitom, D. and Bilong, P. (2015) Caractéristiques

géochimiques des manteaux d'altération sur granitoïdes dans l'Adamaoua (Cameroun). *European Scientific Journal*, **11**, 1857-7881.

[45] Fenske, C., Braun, J., Guillocheau, F. and Robin, C. (2025) A Numerical Model for Duricrust Formation by Water Table Fluctuations. *Earth Surface Dynamics*, **13**, 119-146. https://doi.org/10.5194/esurf-13-119-2025

[46] Steinmann, M. and Stille, P. (2008) Controls on Transport and Fractionation of the Rare Earth Elements in Stream Water of a Mixed Basaltic-Granitic Catchment Basin (Massif Central, France). *Chemical Geology*, **254**, 1-18. https://doi.org/10.1016/j.chemgeo.2008.04.004

[47] Sababa, E., Essomba Owona, L.G., Temga, J.P. and Ndjigui, P. (2021) Petrology of Weathering Materials Developed on Granites in Biou Area, North-Cameroon: Implication for Rare-Earth Elements (REE) Exploration in Semi-Arid Regions. *Heliyon*, **7**, e08581. https://doi.org/10.1016/j.heliyon.2021.e08581

[48] Liu, H., Guo, H., Pourret, O., Wang, Z., Sun, Z., Zhang, W., *et al.* (2021) Distribution of Rare Earth Elements in Sediments of the North China Plain: A Probe of Sedimentation Process. *Applied Geochemistry*, **134**, Article ID: 105089. https://doi.org/10.1016/j.apgeochem.2021.105089

[49] Guo, H., Tuduri, J., Nabyl, Z., Erdmann, S., Li, X. and Gaillard, F. (2024) Rare Earth Elements in Apatite: A Proxy for Unravelling Carbonatite Melt Compositions. *Earth and Planetary Science Letters*, **642**, Article ID: 118863. https://doi.org/10.1016/j.epsl.2024.118863

[50] Akitsu, T. (2013) Ytterbium. In: Kretsinger, R.H., Uversky, V.N. and Permyakov, E.A., Eds., *Encyclopedia of Metalloproteins*, Springer, 2337-2337. https://doi.org/10.1007/978-1-4614-1533-6_200038